12th HSTAM International Congress on Mechanics
Thessaloniki, Greece, 22 – 25 September 2019

MICHELANGELO'S DAVID OR APHRODITE OF MILOS: WHO IS MORE RESISTANT TO BLAST LOADS?

F. Masi[1,2], I. Stefanou[1], P. Vannucci[3], and V. Maffi-Berthier[2]

[1]NAVIER
UMR 8205, École des Ponts, IFSTTAR, CNRS, UPE
Champs-sur-Marne, F-77420, France
e-mail: filippo.masi@enpc.fr , ioannis.stefanou@enpc.fr

[2]Ingérop Conseil et Ingénierie
Rueil-Malmaison, F-92500, France
e-mail: victor.maffi-berthier@ingerop.com

[3]LMV
UMR 8100, Université de Versailles et Saint-Quentin
Versailles, F-78035, France
e-mail: paolo.vannucci@uvsq.fr

Keywords: Blast actions, Rocking motion, Inverted pendulum, Overturning, Museum artefacts.

Abstract. *The resistance of museum artefacts and statues under fast-dynamic excitations arising from explosions is investigated. The study takes root in the existing knowledge and theory of inverted pendulum structures subjected to earthquake loadings and extends them to non-symmetrical pulses due to blast waves.*
Analytical, closed-form solutions for the rocking response and the minimum stand-off distance that must be assured to avoid overturning are determined.

Attention is focused on the response and vulnerability of existing museum artefacts. The analytical findings are used to assess the minimum perimeter around two emblematic statues for protecting them against deliberate explosions.

Direct damage due to the high tensile stresses that develop through the material due to the impact of shock waves is further investigated. For the cases considered, material failure is found to prevail over rocking, hence overturning. The results draw attention on the criticality of preserving these art masterpieces against the explosive threat. The existing protective barriers around the statues of Michelangelo's David and Aphrodite of Milos are found not to satisfactorily secure them against explosions as small as 5 kg.

1 INTRODUCTION

The problem of rocking attracts significant scientific research, mostly in the domain of earthquake engineering (construction of bridges, seismic isolation, masonry structures, historical monuments, etc.). We refer, for instance, to the seminal works of Omori [1, 2] and especially to the investigations of Housner [3], who was the first to study the response of a rigid, free-standing block subjected to constant and square pulse seismic (ground) accelerations. Extensive research has provided useful insights on the dynamic response of a rocking block, see e.g. [4–8].

In the last decades, attention was focused on the (seismic) rocking response of ancient structures such as classical temples and museum artefacts with the aim of preserving such historical masterpieces through the design of seismic isolation devices, see e.g. [9–13].

Herein we extend these studies, investigating the rocking dynamics of museum artefacts and statues under fast-dynamic excitations arising from explosions. Our developments take root in the existing knowledge and theory of inverted pendulum structures subjected to earthquake loadings and extend them to non-symmetrical pulses provoked by blast waves. Assuming a simplified geometry of museum artefacts, we derive moment balance equations and overturning conditions are presented and used to determine the critical (minimum) stand-off distance between the source and the target to prevent toppling. This is accomplished by deriving analytical, closed-form solutions of the minimum stand-off distance that has to be provided to avoid toppling. Our model extends the current understanding of rocking due to blasts (cf. [14–16]) and leads to fundamental insights for design of protective devices.

Fast-dynamic excitations arising from explosions present additional complexity if compared to seismic ones. First, the ultra-high rates involved: the characteristic time of a blast is of several milliseconds instead of $\approx 1 \div 10$ s for earthquakes. Second, wave propagation phenomena and fluid-structure interaction (e.g. diffraction, rarefaction, reflections, etc.) render the characterization of blast loading arduous. The effect of these phenomena

on our modelling assumptions is extensively discussed in [17], where the predictions of our analytical model are compared to detailed numerical analyses that consider the above-mentioned phenomena, a combined sliding/rocking behaviour, and the possibility of uplifting (flight mode).

Engineering applications of the present study can be found in several domains. Of interest here is the preservation of un-anchored equipment and museum (slender) artefacts from overturning, e.g. statues. Such objects belong to the world cultural heritage and their protection has raised important issues throughout history. We refer e.g. to the lost and/or destroyed artefacts of Athena Parthenos, Colossus of Rhodes, the statue of Zeus at Olympia, and more recently the Buddhas statue of Bamiyan. The proposed analytical model can further be used for securing historical buildings made of monolithic columns from collapse (e.g. classical Greek and Roman temples [9, 18]).

The paper is structured as follows. In Section 2 we present the main parameters that identify the blast loading and the model used. We investigate the rocking response and overturning condition for museum artefacts in Section 3. We consider two emblematic statues as case studies for the assessment of protective barriers against overturning due to explosions. In Section 4 the problem of direct damage due to development of important tensile stresses arising from the impinging blast waves is addressed with Finite Element simulations.

2 STATEMENT OF THE PROBLEM AND MODELLING ASSUMPTIONS

The problem of a slender artefact freely standing on a horizontal base is studied considering the target as infinitely rigid. The artefact is modelled as an equivalent rigid rectangular block, with mass m, front surface S equal to the front surface of the artefact and moment of inertia around the pivot point O equal to I_o (computed considering the real geometry of the statue). With reference to Figure 1, the centre of gravity is located at distance r from the pivot point, at a height $h_g = r\ \cos\alpha$ from the ground and width $b = r\ \sin\alpha$. The centroid of the front surface, impinged by the blast wave (simultaneously and uniformly), is at height h_c from the ground (see Fig. 1).

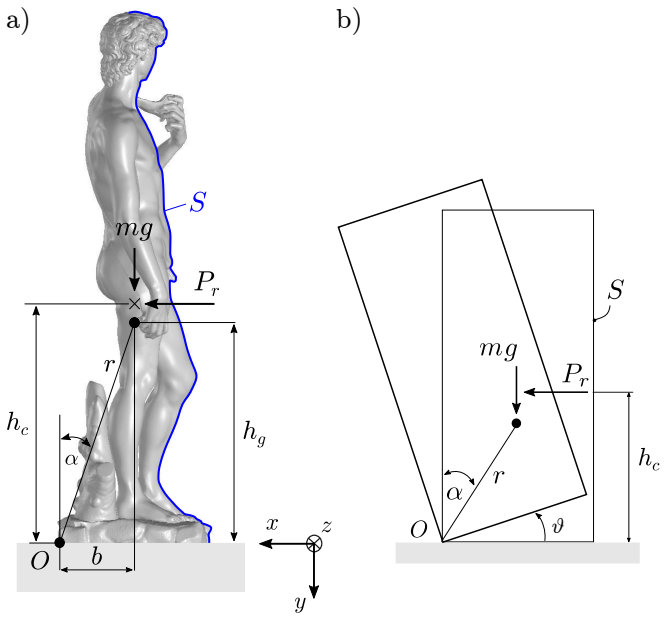

Figure 1. Configuration considered for the rocking problem of museum artefacts: an arbitrarily shaped rigid block (a) and a regular one (b) with rectangular base, resting on a horizontal plane with mass m (centre of gravity at h_g), subjected to a uniform blast pressure applied to surface S (blue), with centroid at h_c.

The contact with the horizontal plane is assumed unilateral and punctual at point O (no contact moment). We further consider the angle of friction at the interface to be sufficiently large to prevent sliding. The pressure load due to the explosion is exclusively applied on the front surface S (incident surface, see Fig. 1) and the blast wave is assumed to act always horizontally (high rates involved) and to impinge all points of S at the same time (simultaneously) and with the same magnitude (uniformly). The fluid-structure interaction phenomena are neglected as well as the effects of induced ground shocks. The corroboration of the validity of the modelling assumptions can be found in [17], where it is shown that the minimum distance that has to be assured between the explosive source and the target, such that toppling is avoided, is in good agreement and on the safety side with the one determined by the full numerical model.

2.1 Blast loading model

Explosion produces a blast wave of high-pressure accompanying high-temperature and supersonic expansion of gases. The abrupt increase of the pressure carried by a blast wave can produce severe structural damage. When the primary shock meets a target, it generates on it the so-called reflected overpressure, P_r, which is the difference between the pressure determined by the explosion increased by the reflection at target's surface and the ambient one, P_o. Figure 2 shows the schematic time variation of P_r, which is determined by the arrival time of the shock wave, t_A, the overpressure peak, P_{ro}, the positive phase duration, t_o, negative phase duration, t_{o-}, and the underpressure peak, P_{ro-}. These parameters are functions of the distance R and the explosive weight (conventionally expressed in TNT equivalent). Herein we consider only the positive phase of the blast wave (safety approach).

The pressure acting on a target due to blast loading is the algebraic sum of the hydrostatic overpressure and the dynamic pressure $C_D\, q := \rho u|u|/2$, with C_D the drag coefficient (function of the target shape and Mach and Reynold numbers), ρ the density, and u the velocity of gas particles.

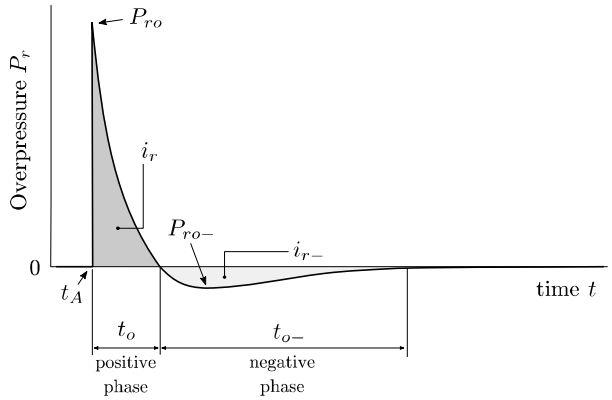

Figure 3. Time evolution of overpressure (i.e. the pressure measured relatively to the atmospheric one) due to an explosion acting on a target.

The simulation of a blast can be conducted by using different approaches [19, 20]. Herein we refer to empirical models based on experimental results available in the existing literature [21] which allow to determine the blast parameters and pressure loading from the knowledge of the trinitrotoluene (TNT) equivalent explosive weight, *W*, and the stand-off distance, *R*. The time evolution of the reflected pressure is modelled with the well-established modified Friedlander equation,

$$P_r(t) = P_{ro}\left(1 - \frac{t}{t_o}\right)(1 - H[t - t_o])\exp\left(-d\frac{t}{t_o}\right), \tag{12}$$

where $H[\cdot]$ denotes the Heaviside (step) function, d is the exponential decay coefficient, and t_A is taken as the origin of the time axis. The impulse i_r associated to the positive phase reads

$$i_r = \int_0^{t_o} P_r(t)\, dt = \left(e^{-d} + d - 1\right)\frac{P_{ro}\, t_o}{d^2}. \tag{13}$$

The drag coefficient C_D is assumed to be equal to 2 (corresponding to a rectangular target) for front surfaces of any shape. We use the empirical predictions of P_{ro} [17], which are valid for rectangular objects. This assumption is on the safety side. For instance, a human body-like shaped target has a drag coefficient $C_D \approx 0.97$–1.43 [22].

3 ROCKING RESPONSE AND OVERTURNING DOMAIN

3.1 Rocking response

From the moment balance around the rocking pivot point *O* and the definition of the dimensionless inclination angle $\phi = \theta/\alpha$ and time $\tau = \wp\, t$ (with $\wp = \sqrt{mgr\,/\,I_o}$), the linearized equation of motion reads

$$\ddot{\phi} = \phi + \chi p\,(1 + \delta) - 1\,, \tag{1}$$

which is valid for small slenderness angles ($\alpha < 20°$) and a unilateral rocking response ($\phi \geq 0$). We refer to [17] for the derivation of the above equation of motion. The angular acceleration is denoted by $\ddot{\phi}$ and

$$\delta = \frac{(h_c - h_g)}{r}, \tag{2}$$

$$\chi = \frac{S}{mg}\frac{P_{ro}}{\alpha}, \tag{3}$$

$$p = \left(1 - \frac{\tau}{\tau_o}\right)(1 - H[\tau - \tau_o]) \exp\left(-d\frac{\tau}{\tau_o}\right). \tag{4}$$

$\chi\ (1+\delta)$ represents the normalized rocking moment, i.e., the ratio between the moment due to the blast load and the restoring moment due to gravity, p the normalized Friedlander time-history, and τ_o the ratio between the characteristic time of the load and the time parameter $\wp$ characterizing the response of the rigid block.

Assuming the block initially at rest ($\phi(0) = 0$, $\dot{\phi}(0) = 0$), Eq. (1) admits a closed-form solution, whose expression in given in [17].

3.2 Overturning condition and domain

Under unilateral excitations, namely the blast positive phase (see Fig. 2), overturning happens when the rocking angle $\theta > \alpha$, i.e., when $\phi > 1$. The overturning criterion is thus found by equating the total work done by the blast loading to the difference in potential energy between positions $\phi = 1$ and $\phi = 0$ (see Housner, [3]).

For slender blocks and in terms of the dimensionless expressions presented above, the overturning condition reads

$$2I\chi\ (1+\delta) \geq 1\,, \tag{5}$$

with $I = \int_0^{\tau_o} p\,\dot{\phi}\,d\tau$ (see [17]). Notice that the left-hand side term in inequality (5) represents the dimensionless overturning moment. The graphical representation of the dimensionless rocking and overturning moments as functions of the stand-off distance is presented in Figure 3 for a rectangular rocking block subjected to the explosion of 1 kg of TNT. The rocking moment, $\chi\ (1+\delta)$, expresses the condition for rocking initiation ($\chi\ (1+\delta) \geq 1$), while the overturning moment, $2I\chi\ (1+\delta)$, reveals the condition for overturning (5).

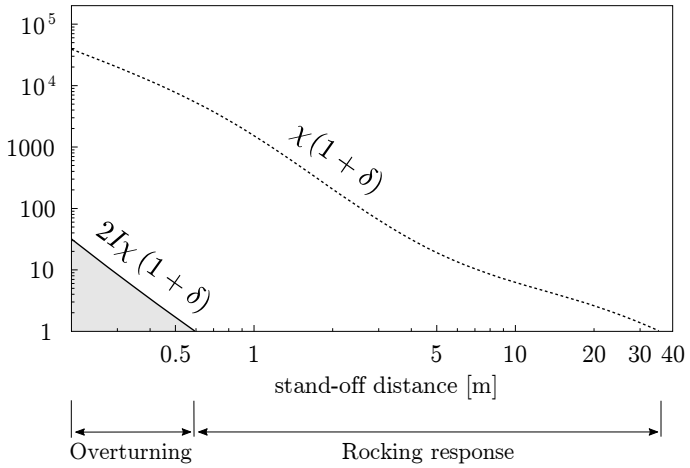

Figure 3. Rocking initiation and overturning condition for a rectangular block with homogeneously distributed mass (i.e. $h_g = h_c$), density 2000 kg/m³, 2 metres high, and $\alpha = 20°$ subjected to 1 kg of TNT at various stand-off distances. The rocking moment, $\chi\ (1+\delta)$, expresses the condition for rocking initiation, i.e. $\chi\ (1+\delta) \geq 1$, while the overturning moment, $2I\chi\ (1+\delta)$, expresses the overturning condition, inequality (5).

From inequality (5), the overturning domain, i.e., the minimum stand-off distance between the explosive source and the target required to avoid toppling, can be derived imposing $2I\chi\ (1+\delta) = 1$. We present in Figure 4 the overturning domain for a rectangular block at varying of the explosive weight, W, and the slenderness angle, α. The critical stand-off distance can be used as a decision-making tool in designing protective perimeters around valuable museum artefacts to avoid their loss due to overturning.

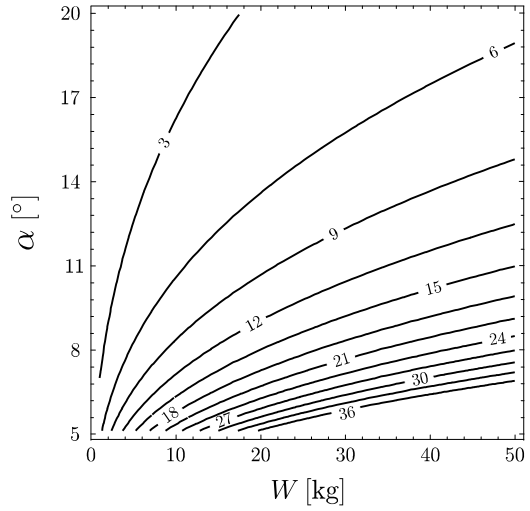

Figure 4. Contours of the critical stand-off distance (in metres) as function of the explosive weight, W, and the slenderness angle, α, for a rectangular museum artefact with homogeneously distributed mass (i.e. $h_g = h_c$), density 2000 kg/m³, 2 metres high, and $\alpha = 20°$.

3.3 Critical stand-off distance of museum artefacts

The corroboration of the above presented overturning domain can be found in a previous study [17], where it is shown that the minimum distance that has to be assured between the explosive source and the target, such that toppling is avoided, is in good agreement and on the safety side with the one determined by the full numerical model.

Herein we investigate the minimum perimeter that has to be assured to prevent the loss, due to overturning, of statues with high aesthetical and historical value in case of a deliberate blast. Two of most emblematic statues of the world cultural heritage are herein considered, see Figure 5. For both statues, the worst-case scenario is assumed: a blast wave with a direction such that the target rocking resistance is the smallest one (minimum slenderness angle and moment of inertia). Table 1 shows the overturning domain of the artefacts for two quantity of explosive (TNT).

Both statues are found to be safely protected with the existing protective barriers (perimeter approximately of 1.50 m). The case of Michelangelo's *David* is particularly interesting. Its large dimensions confer to the statue an excellent resistance to rocking, hence overturning.

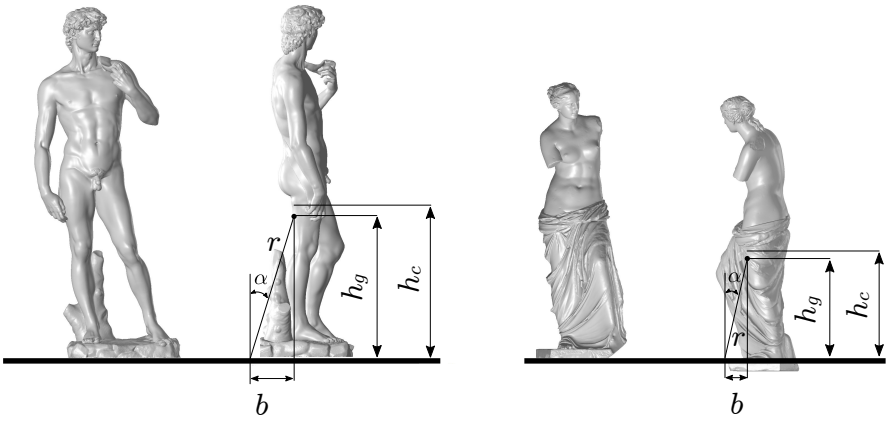

Figure 5. The two museum artefacts considered: Michelangelo's *David* (Gallery of the Academy of Florence, Florence), left, and *Aphrodite of Milos* (Louvre Museum, Paris), right. The three-dimensional models are recovered from the platform Scan The World [23].

Museum artefact	m [kg]	I_o [kg m² ×10³]	h_g [m]	h_c [m]	α [°]	b [m]	S [m²]	Critical stand-off distance [m]			
								W [kg]		10	20
Michelangelo's *David*	5800	1.65×10³	2.28	2.35	17.6	0.7	5.02			0.25	0.32
Aphrodite of Milos	565	16.4	0.86	0.87	18.4	0.28	0.83			0.70	1.0

Table 1: Rocking and overturning parameters for the considered artefacts and corresponding critical stand-off distances for 10 and 20 kg of TNT.

4 RESISTANCE TO DIRECT DAMAGE DUE TO BLAST LOADING

Whilst, for instance, Michelangelo's *David* is safe against toppling due to blast loading, the marble statue may be directly damaged due to the development of important tensile stress.

Once the shock wave impinges the front surface, a compressive wave propagates through the material, with amplitude approximately equal to the overpressure peak, P_{ro} (cf. [24]). Tensile waves further stem from rarefaction phenomena at the free boundaries of the target and interact causing high fluctuations of stress and strain [24, 25, 26]. The stress focalisation may give rise to tensile stresses higher than the material strength, causing hence direct damage of the artefact. Tensile stresses are more likely to damage the marble material with respect to compressive ones, as common geomaterials (such tuff, granite, mortar, etc.) usually display higher strength in compression.

Nevertheless, the tensile strength, f_t, of the material under high strain rates is higher than in quasi-static conditions [27]. Extensive experimental research showed that the loading rate influences the resistance of materials mainly due to the finite growth rate of micro-cracks [28, 29] and the material viscosity [30]. At increasing strain rates, an increase of the tensile strength, among other parameters, is observed, see e.g. [27, 31]. For geomaterials, the dynamic increase factor for tensile strength f_t usually varies between 1, under quasi-static conditions, and 7 in function of the involved strain rates, $\dot{\varepsilon}$, [31]. As far it concerns the museum statues, we refer to marble (namely Carrara marble), whose tensile strength under very low strain rates is f_t = 6.9 MPa and reaches a value of f_t = 50 MPa for strain rates as high as $\dot{\varepsilon}$ = 18 s^{-1} [31].

As the material response is function of the particular geometry of the artefacts and the highly non-linear material behaviour, it is not possible to derive analytical expressions to assess the critical stand-off distance necessary to avoid direct damage due to blast loading. Each case requires ad-hoc investigations through detailed numerical analyses. To this purpose, we perform Finite Element simulations.

For the two museum artefacts considered, during the short time period (≈ 10 ms) following the blast loading, the tensile strength dependency on strain rates $\dot{\varepsilon}$ is negligible as $\dot{\varepsilon} \gg 18$ s^{-1}. We hence assume a constant tensile strength f_t = 50 MPa. The material constitutive law is assumed isotropic, linearly elastic until the maximum principal stress reaches the tensile strength. A subsequent tensile softening is considered in terms of the non-linear brittle cracking model implemented in ABAQUS commercial software [32-34]. In compression, the behaviour is assumed to be linear elastic due to the lower compression stresses involved and the high material strength.

We consider Coulomb friction at the interface between the statue and the rigid base, with an angle of friction φ = 35°, which is common for many geomaterials (concrete, marble, stone, etc.). A hard contact formulation is used, i.e., no penetration is allowed at the contact of the rocking block with the base [32]. Blast loading are applied with ConWep model [35] relying on the best-fit interpolations of the experimental results from Kingery and Bulmash [21].

Table 2 compares the critical stand-off distances to avoid overturning (according to the analytical model presented in Sect. 3) and direct damage (obtained through numerical Finite Element simulations) for the statues of Michelangelo's *David* and *Aphrodite of Milos*. Figure 6 displays the time evolution of the maximum principal stress developed within the statue of *Aphrodite of Milos* and the subsequent material damage due to 10 kg of TNT at 2 metres from the target. The non-standard, fine geometry of the artefact gives rise to strong stress concentrations. At time t = 300 μs after the shock arrival, damage appears in the lower part of the body and propagates within. As the stress waves travel through the material, the reflection and localisation of stress waves at the level of the neck takes place and causes its breakage (t = 900 μs). Even if the statue is found to be safe against overturning, due to the interaction between the geometry and the material stress waves, the existing protective perimeter around *Aphrodite of Milos*, at Louvre Museum (Paris), is insufficient to the preservation against explosions as small as 5 kg (corresponding to a critical stand-off distance ≈ 1.7 m). Whilst the statue of the *David* is more resistance against overturning with respect to *Aphrodite*, its geometry and stress state under self-weight render it more vulnerable to deliberate explosions (direct damage).

Museum artefact	Critical stand-off distance [m]			
	overturning		direct damage	
W [kg]	10	20	10	20
Michelangelo's David	0.25	0.32	2.95	3.90
Aphrodite of Milos	0.70	1.0	2.12	2.67

Table 2: Comparison of the critical stand-off distance to avoid overturning and direct damage for the statues of Michelangelo's David and Aphrodite of Milos.

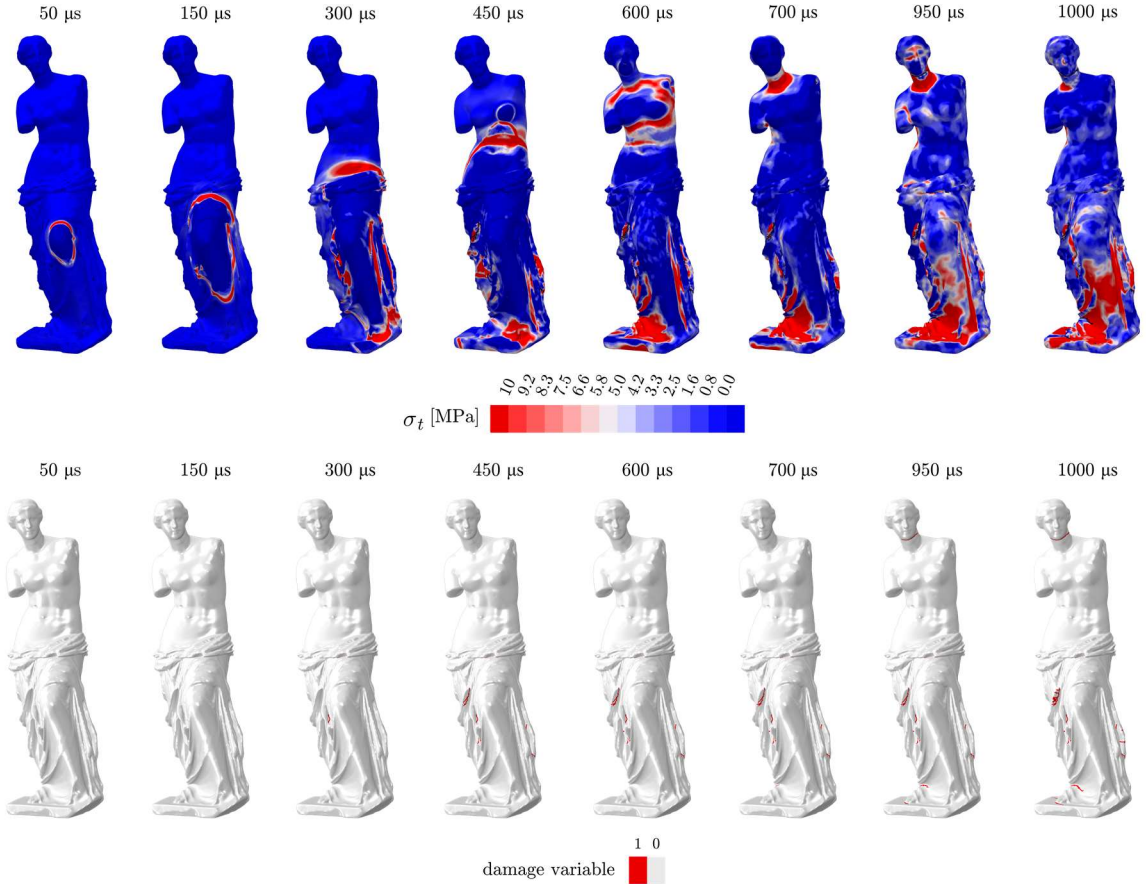

Figure 6. Time evolution of the maximum principal stress (top) and material damage (bottom) for the statue of Aphrodite of Milos due to 10 kg of TNT at 2 metres from the target. Finite elements undergoing damage correspond to a unit damage variable.

6 CONCLUDING REMARKS

We investigated the resistance of museum artefacts, modelled as inverted pendulum structures, under fast-dynamic excitations arising from an explosion. First, by virtue of a simplified expression of blast actions and based on established empirical models, we derived the equations of motion for the rocking of museum artefacts. The overturning condition was then presented and used to derive the minimum distance (critical stand-off distance) that has to be assured between the explosive source and the target, such that toppling is avoided. The proposed analytical model was corroborated in a previous study [17] by detailed numerical simulations accounting for a combined rocking/sliding behaviour, the possibility of uplifting (flight mode), and the complex fluid-structure interaction phenomena. Second, we assessed the overturning domain of two of the most emblematic statues belonging to the world cultural heritage: Michelangelo's *David* and *Aphrodite of Milos*.

Finally, direct material damage due to the development of tensile stresses within the body of the targets impinged by the shock wave was investigated. The highly non-linear material behaviour as well as the complex interaction between the artefact and the material stress waves render not viable a theoretical treatment of the problem of direct damage due to blast loading. Ad-hoc investigations were therefore presented and used to assess the critical strand-off distance to avoid direct (material) damage for the statues of *David* and *Aphrodite of Milos*. For both cases, the non-standard geometry of the target gives rise to strong stress concentrations which render the structure more vulnerable to damage rather than overturning.

REFERENCES

[1] Omori F (1900). Seismic experiments on the fracturing and overturning of columns, Publications of the Earthquake Investigation Committee in Foreign Language 4, 69–141.

[2] Omori F (1902). On the overturning and sliding of columns, Publications of the Earthquake Investigation Committee in Foreign Language 12, 8–27.

[3] Housner GW (1963). The behavior of inverted pendulum structures during earthquakes, Bulletin of the seismological society of America 53(2), 403–417.

[4] Zhang J, Makris N (2001). Rocking response of free-standing blocks under cycloidal pulses, Journal of Engineering Mechanics 127(5), 473–483.

[5] Voyagaki E, Psycharis IN, Mylonakis G (2013). Rocking response and overturning criteria for free standing rigid blocks to single—lobe pulses, Soil Dynamics and Earthquake Engineering 46, 85–95.

[6] Dimitrakopoulos EG, DeJong MJ (2012). Revisiting the rocking block: closed-form solutions and similarity laws, Proceedings of the Royal Society of London A: Mathematical, Physical and Engineering Sciences 468(2144), 2294–2318.

[7] Peña F, Prieto F, Lourenço PB, Campos Costa A, Lemos JV (2007). On the dynamics of rocking motion of single rigid-block structures, Earthquake Engineering & Structural Dynamics 36(15), 2383–2399.

[8] Konstantinidis D, Makris N (2010). Experimental and analytical studies on the response of 1/4-scale models of freestanding laboratory equipment subjected to strong earthquake shaking, Bulletin of Earthquake Engineering 8(6), 1457–1477.

[9] Konstantinidis D,Makris N (2005). Seismic response analysis of multi-drum classical columns. Earthquake Engineering and Structural Dynamics 34, 1243–1270.

[10] Koumousis V (2007). Design of the seismic isolation system for the statue of Hermes at the New museum of Olympia (paper & presentation). Electronic publication. Istanbul, Anti-Seismic Systems International Society.

[11] Stefanou I, Vardoulakis I, Mavraganis A (2011). Dynamic motion of a conical frustum over a rough horizontal plane. International Journal of Non-Linear Mechanics 46(1), 114-124.

[12] Vassiliou MF, Makris N (2012). Analysis of the rocking response of rigid blocks standing free on a seismically isolated base. Earthquake Engineering & Structural Dynamics 41(2), 177-196.

[13] Kounadis AN (2014). Rocking instability under ground motion of large statues freely standing atop elastically supported cantilevers. Archive of Applied Mechanics 84(7), 933–951.

[14] Custard GH, Thayer JR (1970). Target response to explosive blast, Tech. Rep., Falcon Research and Development, U.S. Department of Defense.

[15] Baker WE, Kulesz JJ, Ricker RE, Bessey RL, Westine PS, Parr VB, Oldham GA (1975). Workbook for predicting pressure wave and fragment effects of exploding propellant tanks and gas storage vessels, Tech. Rep., NASA, United States, 1975.

[16] Scherbatiuk K, Rattanawangcharoen N (2008). Experimental testing and numerical modeling of soil-fled concertainer walls, Engineering Structures 30(12), 3545–3554.

[17] Masi F, Stefanou I, Vannucci P, Maffi-Bertier V (2019). Rocking response and overturning of museum artefacts due to blast loading. Proceedings of the 7th ECCOMAS Thematic Conference on Computational Methods in Structural Dynamics and Earthquake Engineering (COMPDYN 2019), Papadrakakis, Fraiadakis (eds), Crete, Greece, 24–26 June.

[18] Stefanou I, Psycharis I, Georgopoulos IO (2011). Dynamic response of reinforced masonry columns in classical monuments. Construction and Building Materials 25(12), 4325-4337.

[19] Remennikov AM (2003). A review of methods for predicting bomb blast effects on buildings, Journal of Battlefield Technology 6, 5–10.

[20] Larcher M, Casadei F (2010). Explosions in Complex Geometries - A Comparison of Several Approaches, International Journal of Protective Structures 1(2), 169–195.

[21] Kingery CN, Bulmash G (1984). Air blast parameters from TNT spherical air burst and hemispherical burst, Tech. Rep., U.S. Army Ballistic Research Laboratory.

[22] Penwarden AD, Grigg PF, Rayment R (1978). Measurements of wind drag on people standing in a wind tunnel, Building and environment 13(2), 75–84.

[23] MyMiniFactory, Scan The World, London, UK.

[24] Meyers MA (1994). Dynamic behavior of materials, John Wiley & Sons.

[25] Vales F, Moravka S, Brepta R, Cerv J (1996). Wave propagation in a thick cylindrical bar due to longitudinal impact, JSME Mechanics and Material Engineering 39(1), 60–70.
[26] Gu X, Zhang Q, Huang D, Yv Y (2016). Wave dispersion analysis and simulation method for concrete SHPB test in peridynamics, Engineering Fracture Mechanics 160, 124–137.
[27] Ross CA, Tedesco JW, Kuennen ST (1995). Effects of strain rate on concrete strength, Materials Journal 92 (1), 37-47.
[28] Freund L (1972). Crack propagation in an elastic solid subjected to general loading—i. constant rate of extension, Journal of the Mechanics and Physics of Solids 20(3), 129–140.
[29] Freund L (1972). Crack propagation in an elastic solid subjected to general loading—II. non-uniform rate of extension, Journal of the Mechanics and Physics of Solids 20(3),141–152.
[30] Weerheijm J (1992). Concrete under impact tensile loading and lateral compression, Ph.D. thesis, TU Delft, Delft University of Technology.
[31] Wong LNY, Zou C, Cheng Y (2014). Fracturing and failure behavior of carrara marble in quasistatic and dynamic Brazilian disc tests, Rock Mechanics and Rock Engineering 47(4), 1117–1133.
[32] ABAQUS (2016). Abaqus analysis user's guide, Tech. Rep. Abaqus 6.14 Documentation, Simulia Corp.
[33] Hillerborg A, Modéer M, Petersson PE (1976). Analysis of crack formation and crack growth in concrete by means of fracture mechanics and finite elements, Cement and Concrete Resistance 6, 773–782.
[34] Masi F, Stefanou I, Vannucci P (2018). A study on the effects of an explosion in the Pantheon of Rome, Engineering Structures 164, 259–273.
[35] Hyde D (1993). Conwep: Conventional weapons effects program, US Army Engineer Waterways Experiment Station, USA.